Supplementary Information

Lure the "Enemy" Deep: An Innovative Biomimetic Strategy for Enhancing the Microwave Absorption Performance of Carbon Nanofibers

Yu Deng [a], Minghang Yang [a], Yining Wang [a], Mingguang Zhang [a], Shuaining Zhou [a], Xiangyang Lu [a], Xigao Jian [a], Yousi Chen [a*]

[a] State Key Laboratory of Fine Chemicals, Frontiers Science Center for Smart Materials Oriented Chemical Engineering, Liaoning Technology Innovation Center of High Performance Resin Materials, Dalian Basalt Fiber Resin Matrix Composite Engineering Research Center, Department of Polymer Science & Engineering, Dalian University of Technology, Dalian 116024, P.R. China.

Corresponding Author E-mail: **chenyousi@dlut.edu.cn**

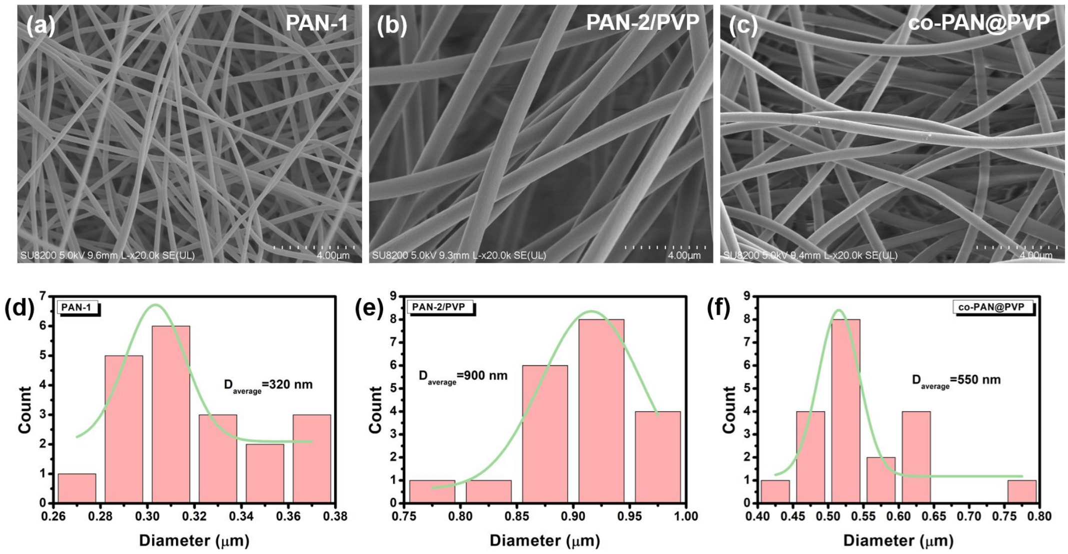

Fig. S1 SEM images and diameter distribution of NFs: (a, d) PAN-1; (b, e) PAN-2/PVP; (c, f) co-PAN@PVP.

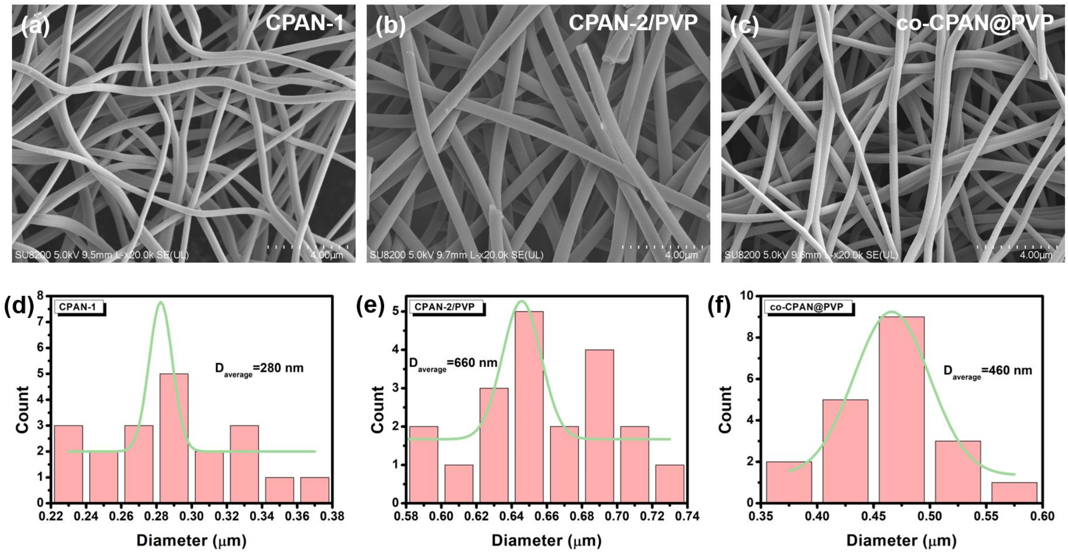

Fig. S2 SEM images and diameter distribution of CNFs: (a, d) CPAN-1; (b, e) CPAN-2/PVP; (c, f) co-CPAN@PVP.

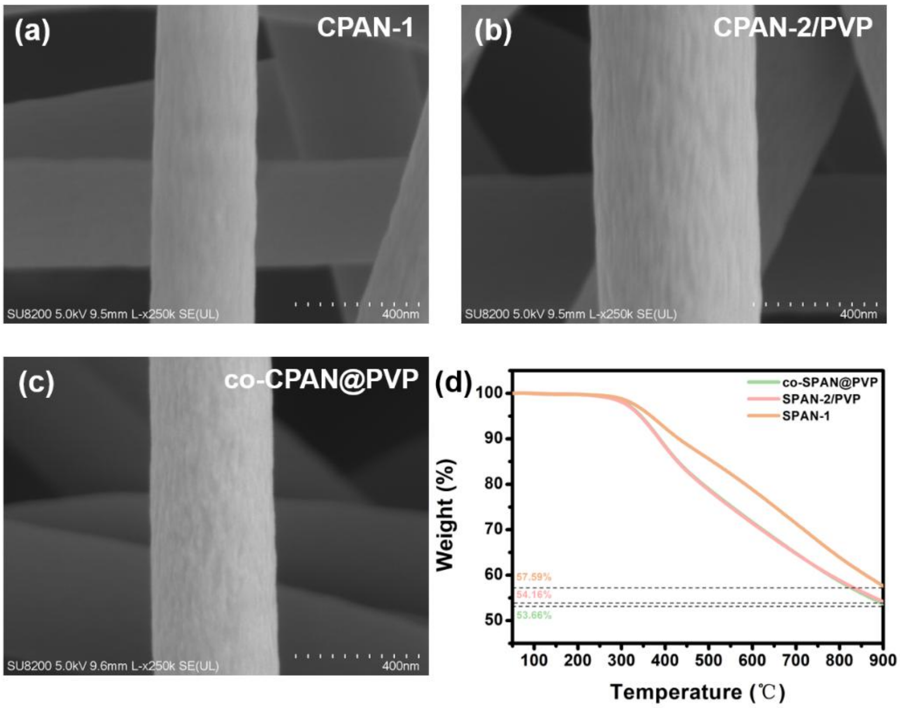

Fig. S3 Surface morphology of CNFs: (a) CPAN-1; (b) CPAN-2/PVP; (c) co-CPAN@PVP and (d) TGA curves.

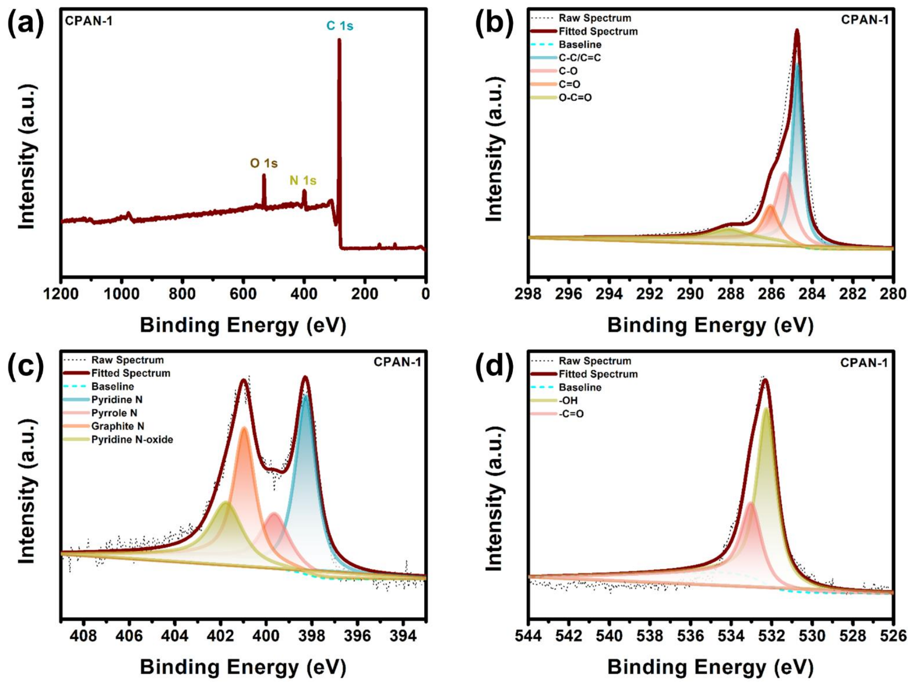

Fig. S4 (a) XPS survey spectra and (b) C 1s, (c) N 1s, and (d) O 1s spectra of CPAN-1.

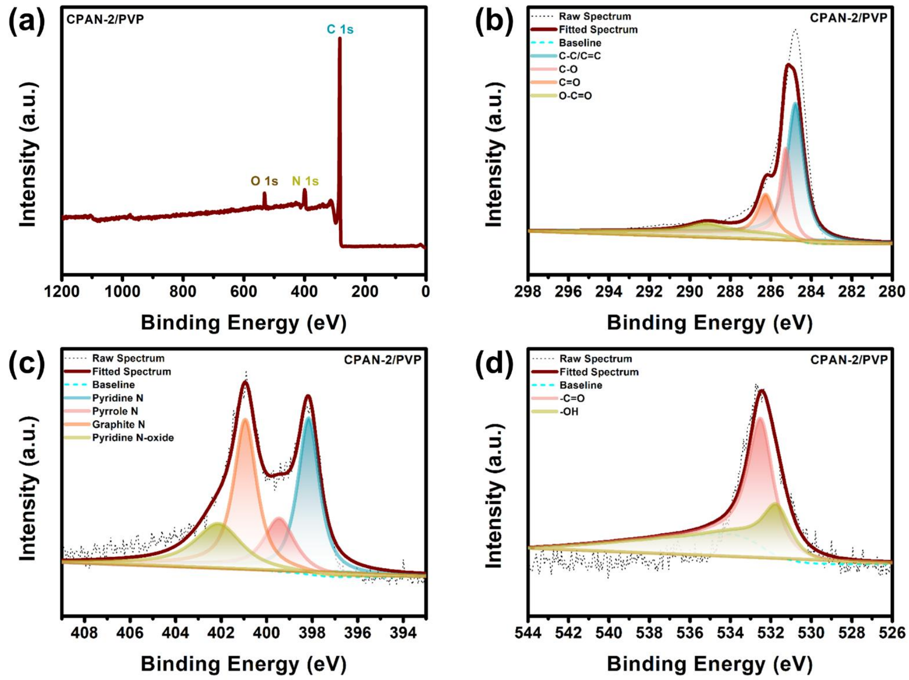

Fig. S5 (a) XPS survey spectra and (b) C 1s, (c) N 1s, and (d) O 1s spectra of CPAN-2/PVP.

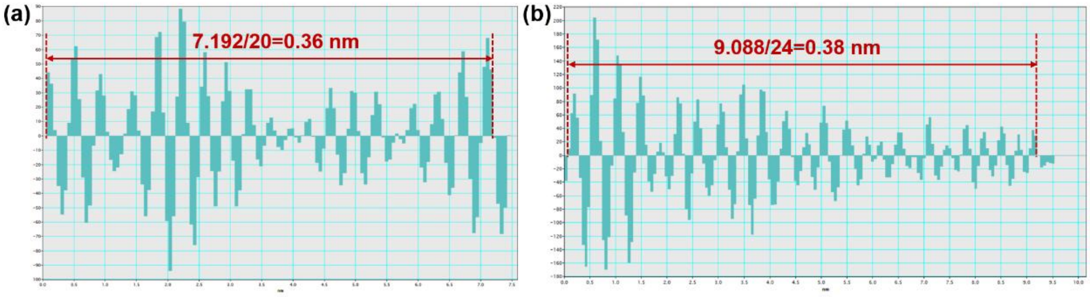

Fig. S6 Calculation of TEM crystal plane spacing: (a) CPAN-1; (b) CPAN-2/PVP.

Table S1 Diameter shrinkage rate of NFs after carbonization

Samples	Shrinkage rate (%)
CPAN-1	12.5
CPAN-2/PVP	26.7
co-CPAN@PVP	16.4

The interlayer distance (d_{002}) and stacking layer thickness (L_c) of graphite grains were calculated according to formulas (S1) and (S2):[1]

$$d_{002} = \frac{K\lambda}{2\sin\theta} \tag{S1}$$

$$L_c = \frac{K\lambda}{\beta\cos\theta} \tag{S2}$$

where K is the shape factor with a value of 0.9, λ is the wavelength of the CuKα X-ray (0.15046 nm), and β is the maximum half width at half maximum (FWHM) of the diffraction peak at 2θ.

Table S2 The interlayer spacing and stacking layer thickness of CNFs

Samples	2θ (degree)	d_{002} (nm)	L_c (nm)
CPAN-1	21.30	0.3664	1.353
CPAN-2/PVP	21.17	0.3686	1.308
co-CPAN@PVP	20.76	0.3758	1.292

The average distance between defects (L_d) and defect density (n_d) of materials can be calculated as follows:[2]

$$L_d\,(\text{nm}) = \sqrt{(1.8 \pm 0.5) \times 10^{-9} \lambda_L^4 (\frac{I_D}{I_G})^{-1}} \tag{S3}$$

$$n_d\,(\text{cm}^{-2}) = \frac{(1.8 \pm 0.5) \times 10^{22}}{\lambda_L^4} (\frac{I_D}{I_G}) \tag{S4}$$

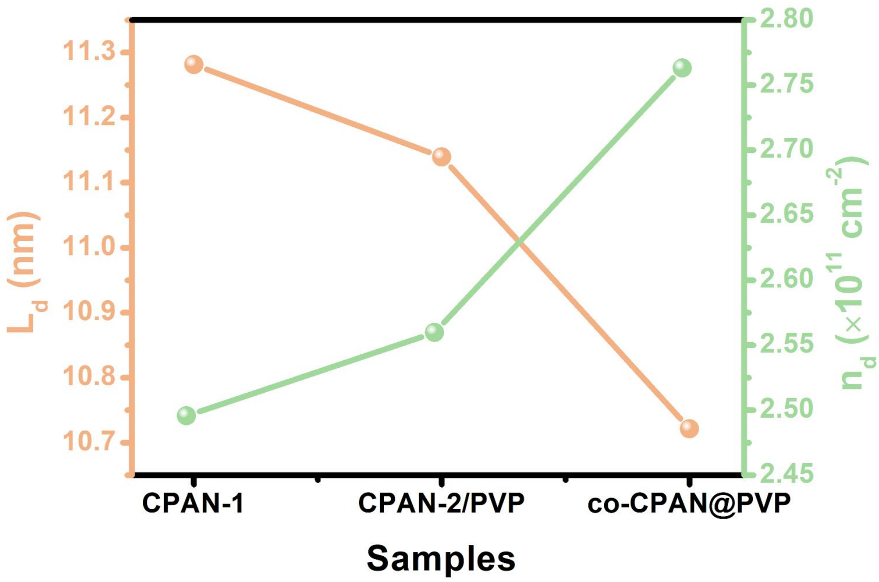

Fig. S7 Average L_d and n_d of CNFs.

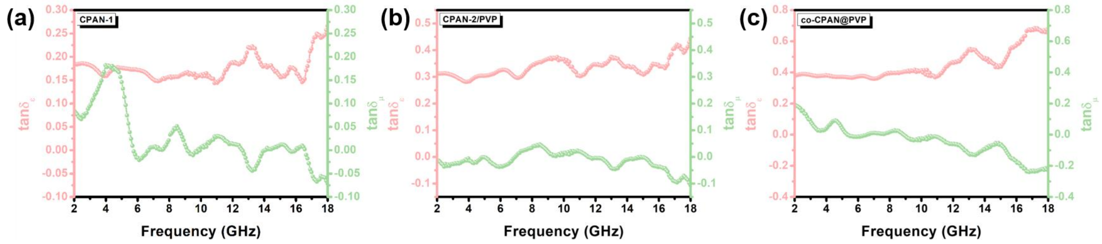

Fig. S8 Comparison of dielectric loss and magnetic loss: (a) CPAN-1; (b) CPAN-2/PVP; (c) co-CPAN@PVP.

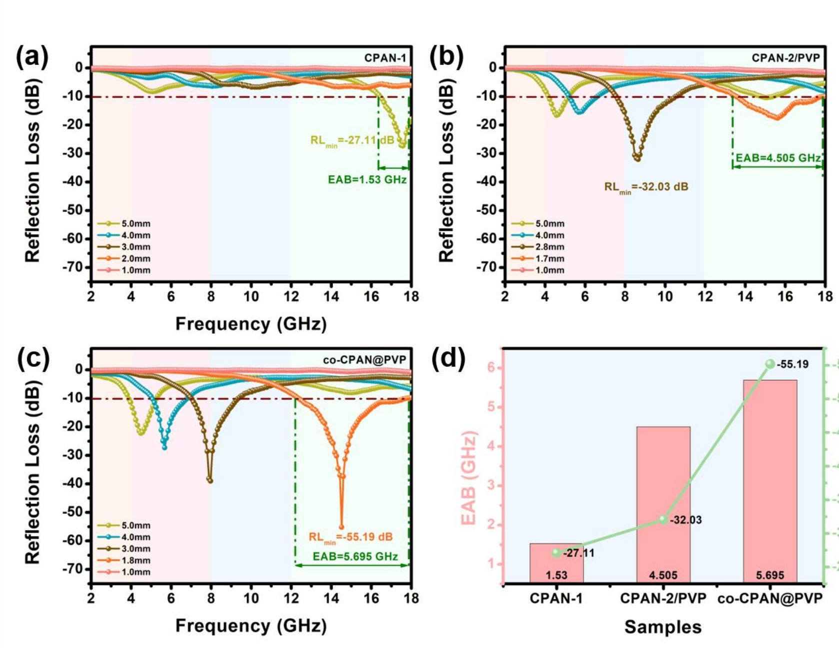

Fig. S9 The RL_{min} value at a given thickness of (a) CPAN-1, (b) CPAN-2/PVP and (c) co-CPAN@PVP; (d) Comparison of absorption performance.

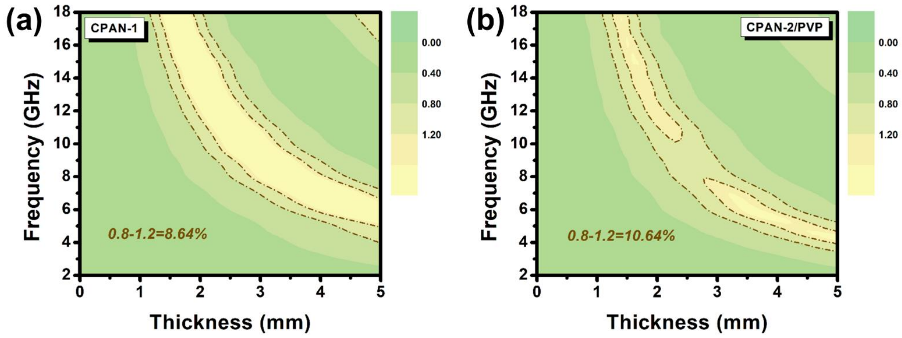

Fig. S10 Z of (a) CPAN-1 and (b) CPAN-2/PVP.

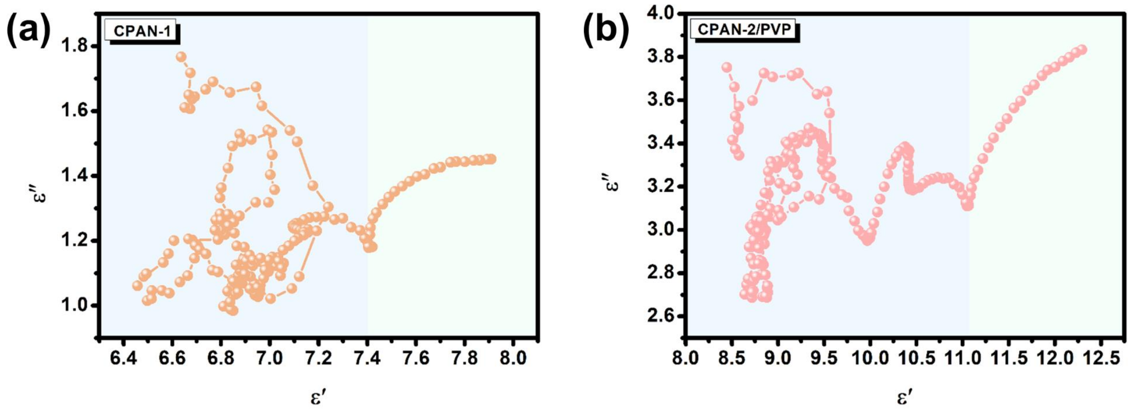

Fig. S11 Cole-Cole curves: (a) CPAN-1; (b) CPAN-2/PVP.

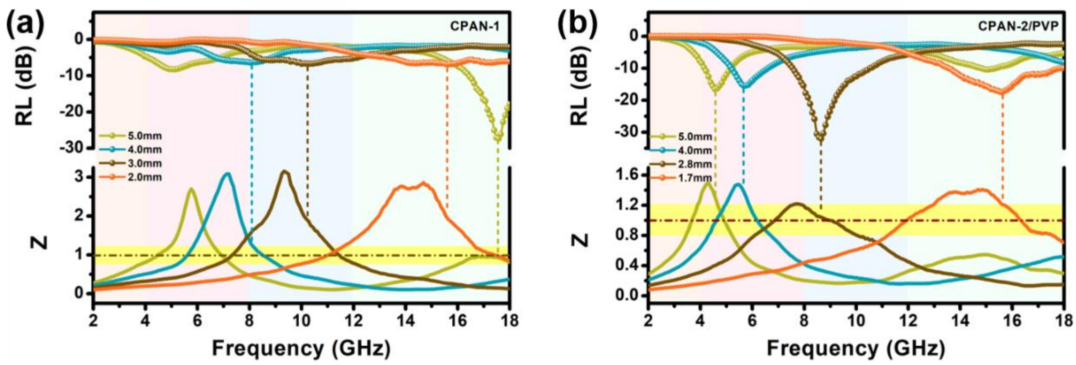

Fig. S12 RL and Z corresponding curves: (a) CPAN-1; (b) CPAN-2/PVP.

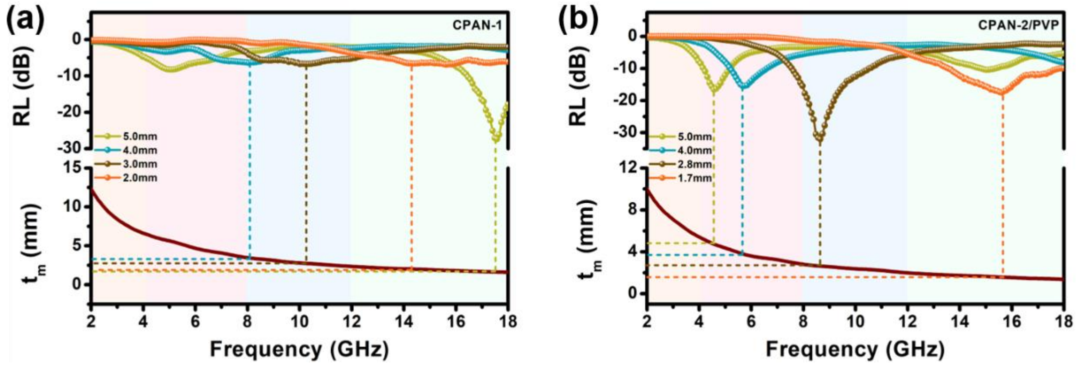

Fig. S13 RL and t_m corresponding curves: (a) CPAN-1; (b) CPAN-2/PVP.

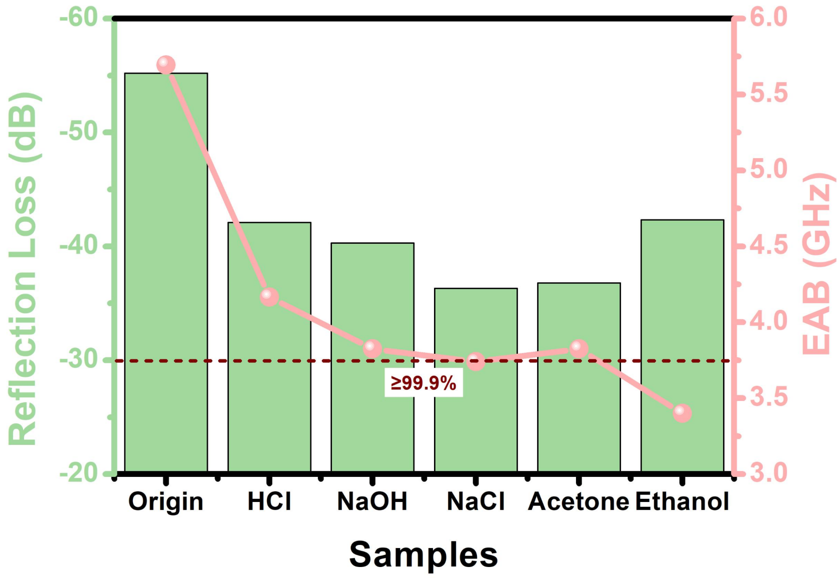

Fig. S14 The absorption performance of co-CPAN@PVP in harsh environments.

$$SRL_1 = \frac{|RL_{\min}|}{loading * d} \tag{S5}$$

$$SEAB_1 = \frac{EAB}{loading * d} \tag{S6}$$

$$SRL_1 = \frac{|RL_{\min}|}{loading} \tag{S7}$$

$$SEAB_l = \frac{EAB}{loading} \tag{S8}$$

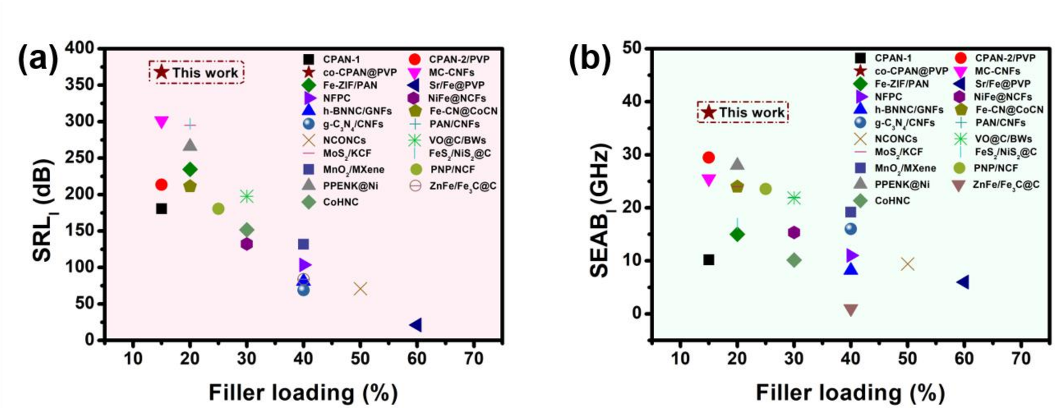

Fig. S15 Comparison of absorption performance of carbon-based MAMs in recent years.

Table S3 Comparison of MA performance of carbon-based MAMs in recent years

Samples	RL (dB)	d_1 (mm)	EAB (GHz)	d_2 (mm)	loading (wt.%)	Ref.
CPAN-1	-27.11	5	1.53	5	15	This work
CPAN-2/PVP	-32.03	2.8	4.42	1.7	15	This work
co-CPAN@PVP	-55.19	1.8	5.695	1.8	15	This work
MC-CNFs	-45.19	2.8	3.825	2.8	15	3
Fe-ZIF/PAN	-46.9	2	3	2	20	4
Sr/Fe@PVP	-12.69	3.4	3.6	2	60	5
NFPC	-41.4	1.36	4.4	1.34	40	6
NiFe@NCFs	-39.7	2	4.6	1.45	30	7
h-BNNC/GNFs	-32.28	2	3.28	2	40	8
Fe-CN@CoCN	-42.27	2.5	4.8	2.5	20	9
g-C_3N_4/CNFs	-27.56	2.3	6.4	2.3	40	10
PAN/CNFs	-44.73	1.76	6.6	1.76	30	11
NCONCs	-35.47	1.4	4.71	1.4	50	12
VO@C/BWs	-59.3	2.34	6.56	2.34	30	13
MoS_2/KCF	-59	2.5	4.8	2.5	20	14
FeS_2/NiS_2@C	-59.4	3.2	3.4	2	20	15
MnO_2/MXene	-52.74	2.9	7.68	2.9	40	16
PNP/NCF	-45.1	3.6	5.89	2	25	17
PPENK@Ni	-53.2	1.5	5.6	1.5	20	18
ZnFe/Fe_3C@C	-33.57	1.5	4.16	1.34	40	19
CoHNC	-45.5	1.4	3.04	1.4	30	20

$$\varepsilon^{'} = \varepsilon_{\infty} + \frac{\varepsilon_s - \varepsilon_{\infty}}{1+\omega^2\tau^2} \quad \text{(S9)}$$

$$\varepsilon^{"} = \frac{\varepsilon_s - \varepsilon_{\infty}}{1+\omega^2\tau^2}\omega\tau + \frac{\sigma}{\omega\varepsilon_0} = \varepsilon_p^{"} + \varepsilon_c^{"} \quad \text{(S10)}$$

where ω is the angular frequency, τ is the polarization relaxation time, ε_s is the static permittivity, ε_∞ stands for the dielectric permittivity at the high frequency limit and σ is the electric conductivity.[21]

$$E_a = E_1 + E_2 \quad \text{(S11)}$$

$$E_1 = \pi f \varepsilon^{'} E_0^2 + \pi f \mu^{'} H_0^2 \quad \text{(S12)}$$

$$E_2 = \pi f \varepsilon^{"} E_0^2 + \pi f \mu^{"} H_0^2 \quad \text{(S13)}$$

where E_a is the absorbed incident EM energy, E_1 and E_2 represent the energy of storage and conversion part, E_0 and H_0 are the electric and magnetic field intensity amplitude of electromagnetic wave, respectively.[22]

$$w_s = \frac{E_1}{E_1 + E_2} \quad \text{(S14)}$$

$$w_d = \frac{E_2}{E_1 + E_2} \quad \text{(S15)}$$

$$w_r = \frac{E_2}{E_1} \quad \text{(S16)}$$

where w_s is the electromagnetic energy storage efficiency, w_d is the conversion efficiency and w_r is the ratio of electromagnetic wave conversion to storage.

$$E_{2p} = \pi f \varepsilon_p^{"} E_0^2 \quad \text{(S17)}$$

$$E_{2c} = \pi f \varepsilon_c^{"} E_0^2 \quad \text{(S18)}$$

$$E_{2m} = \pi f \mu^{"} H_0^2 \quad \text{(S19)}$$

where E_{2p}, E_{2c} and E_{2m} represent conversion energy contributed by polarization, conductive and magnetic losses.

$$w_p = \frac{E_{2p}}{E_{2c} + E_{2p} + E_{2m}} \quad \text{(S20)}$$

$$w_c = \frac{E_{2c}}{E_{2c} + E_{2p} + E_{2m}} \tag{S21}$$

$$w_m = \frac{E_{2m}}{E_{2c} + E_{2p} + E_{2m}} \tag{S22}$$

where w_p, w_c and w_m represent the efficiency of converted EM energy by conductance, relaxation and magnetic mechanism.

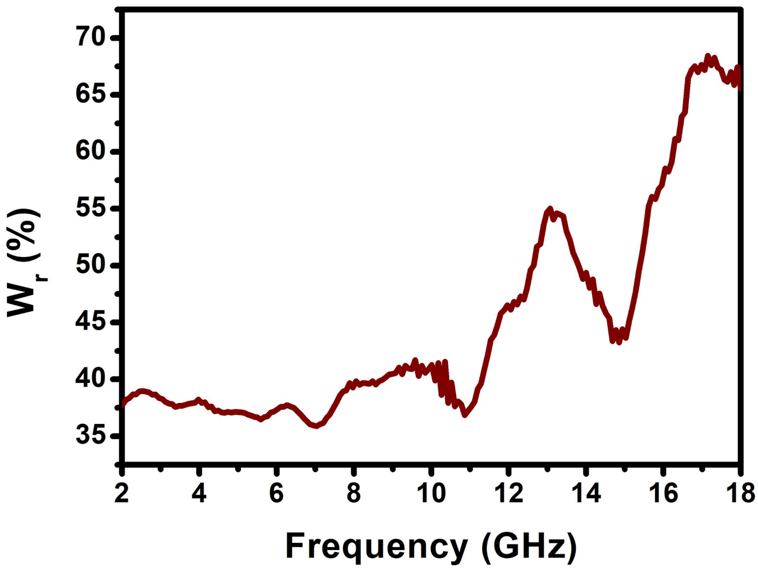

Fig. S16 Microwave conversion efficiency to storage efficiency ratio for co-CPAN@PVP.

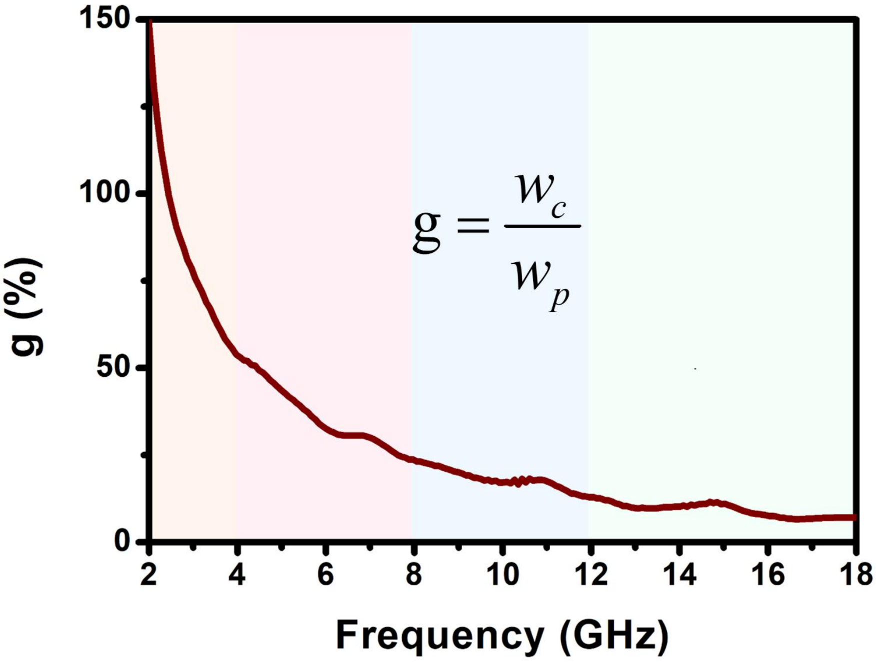

Fig. S17 The ratio (g) of EM energy conversion power contributed by charge transport and relaxation (w_c and w_p).

References

1. M. Yang, L. Sun, Q. Liu, Y. Deng, C. Liu, N. Li, J. Xu, Y. Chen and X. Jian, *Polym. Adv. Technol.*, 2024, **35**, e6300.
2. J. Yu, H. Luo, Z. Wang, S. Lv, Y. Cheng, F. Chen, S. Yan and X. Li, *J. Alloys Compd.*, 2024, **971**, 172757.
3. Y. Deng, M. Yang, Q. Liu, C. Liu, X. Jian and Y. Chen, *ACS Appl. Nano Mater.*, 2024, **7**, 3199-3209.
4. R. Sun, G. Yan, X. Zhang, Z. Li, J. Chen, L. Wang, Y. Wu, Y. Wang and H. Li, *Chem. Eng. J.*, 2023, **455**, 140608.
5. Z. Wang, L. Zhao, P. Wang, L. Guo and J. Yu, *J. Alloys Compd.*, 2016, **687**, 541-547.
6. S. Lv, H. Luo, Z. Wang, J. Yu, Y. Cheng, F. Chen and X. Li, *Carbon*, 2024, **218**, 118668.
7. F. Chen, S. S. Zhang, R. D. Guo, B. B. Ma, Y. Xiong, H. Luo, Y. Z. Cheng, X. Wang and R. Z. Gong, *Compos. Pt. B-Eng.*, 2021, **224**, 109161.
8. B. Zhong, W. Liu, Y. Yu, L. Xia, J. Zhang, Z. Chai and G. Wen, *Appl. Surf. Sci.*, 2017, **420**, 858-867.
9. S. Ren, P. Ju, H. Yu, B. Nan, L. Wang, A. Lian, X. Zang and H. Liang, *Coatings*, 2024, **14**, 133.
10. K. Yang, B. Fan, Y. Yang, S. Cai, M. Ying, X. Wang, G. Tong, W. Wu and D. Chen, *Carbon*, 2024, **219**, 118849.
11. J. Xiao, B. Zhan, M. He, X. Qi, X. Gong, J. L. Yang, Y. Qu, J. Ding, W. Zhong and J. Gu, *Adv. Funct. Mater.*, 2024, 2316722.
12. Y. Guo, H. Lu and X. jian, *Ceram. Int.*, 2024, **50**, 8030-8041.
13. A. Ni, Z. Xiong, Y. Zhang, X. Jiang, X. Li, C. Liu and X. Zeng, *Carbon*, 2024, **221**, 118930.
14. X. Wang, X. Cao, E. Ding, M. Yin, L. Huang and L. Zhang, *Carbon*, 2024, **221**, 118887.
15. J. Wang, Y. Wang, W. Wang and K. Nan, *Carbon*, 2024, **218**, 118735.
16. S. Chen, Y. Meng, X. Wang, D. Liu, X. Meng, X. Wang and G. Wu, *Carbon*, 2024, **218**, 118698.
17. H. Xu, M. Liu, Z. Ma, B. Kang, X. Zhang, C. Zhu, X. Zhang and Y. Chen, *Chem. Eng. J.*, 2024, **479**, 147666.
18. C. Wang, L. Zong, Y. Pan, N. Li, Q. Liu, J. Wang and X. Jian, *Compos. Pt. B-Eng.*, 2021, **223**, 109114.
19. R. Guo, D. Su, K. Zou, C. Zhang, F. Cen, H. Luo, F. Chen and S. Jiang, *ACS Appl. Nano Mater.*, 2021, **4**, 11070-11079.
20. X. Han, S. Zhang, L. Qiao, P. Peng, C. Fu, K. Liu and Z. Ma, *ACS Appl. Nano Mater.*, 2024, **7**, 5414-5425.
21. T. Liu, Q. Zheng, W. Cao, Y. Wang, M. Zhang, Q. Zhao and M. Cao, *Advanced Composites and Hybrid Materials*, 2024, **7**.
22. Q. Wang, B. Niu, Y. Han, Q. Zheng, L. Li and M. Cao, *Chem. Eng. J.*, 2023, **452**.